

Controllable, intense spectral peaking with a spectral filter and optical fiber: supplement

NORHIKO NISHIZAWA,*  SAKIKO KOBATA, AND SHOTARO KITAJIMA 

Department of Electronics, Nagoya University, Furo-cho, Chikusa-ku, Nagoya 464-8603, Japan

**Corresponding author: nishizawa@nuee.nagoya-u.ac.jp*

This supplement published with Optica Publishing Group on 23 November 2022 by The Authors under the terms of the [Creative Commons Attribution 4.0 License](https://creativecommons.org/licenses/by/4.0/) in the format provided by the authors and unedited. Further distribution of this work must maintain attribution to the author(s) and the published article's title, journal citation, and DOI.

Supplement DOI: <https://doi.org/10.6084/m9.figshare.21498192>

Parent Article DOI: <https://doi.org/10.1364/OL.471957>

Controllable, intense spectral peaking with spectral filter and optical fiber: supplemental document

S1. Characteristics of spectral peaking by spectral intensity filter

Here we discuss the characteristics of spectral peaking by spectral intensity filter.

Figure S1(a) shows the variation of optical spectra when the spectral intensity filter was applied. The conditions of the input pulse were the same as those in Fig. 2. The spectral envelope was broadened through SPM, and the sharp spectral peak with good SBR was generated. From Fig. S1(a), the gain for the spectral peak was almost 1.05. It was considered that the initial spectral dip component was appeared as the spectral peak on the spectral envelope.

Figure S2(b) shows the variation of the spectral peak power for the phase and intensity filtering as a function of the modulation pixel number. The ND-HNLF was used as the sample fiber.

As the pixel number was increased, the power of spectral peak was increased and took maximum when the pixel number was 8, and then decreased. The power of spectral peak for phase filtering was about 3 times as large as that of the intensity filtering. We confirmed that the phase filtering is much effective to generate intense spectral peaks.

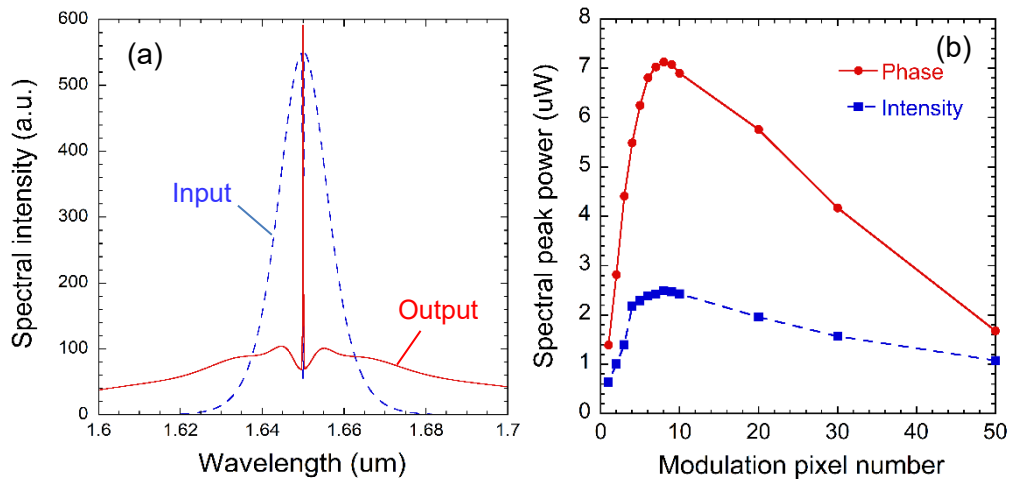


Fig. S1 (a) Input spectra and 1st peak for intensity filtering. (b) variation of spectral peak power as a function of modulation lines when phase modulation (red solid line) and intensity modulation (blue broken one) are applied.

S2. Characteristics of spectral peaks in temporal domain

In order to discuss the physical mechanism of intense spectral peak generation with small background, we discuss the characteristics of spectral peak generation in temporal domain.

Figure S2(a) shows the corresponding temporal waveform and instantaneous wavelength for the 1st peak generation. The temporal shape of ultrashort pulse is slightly broadened to 450 fs, and the linear chirping by normal dispersion is observed.

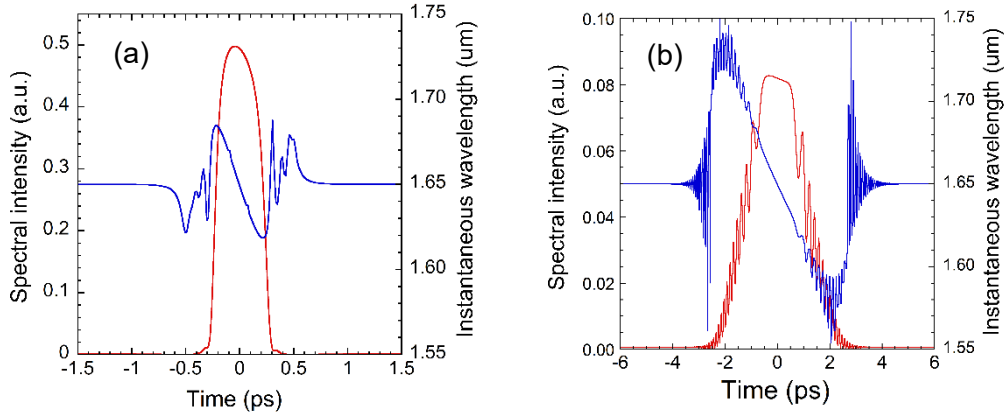


Fig. S2 Temporal shape (red lines) and instantaneous wavelength (blue ones) corresponding to Fig. 4 when (a) 1st and (b) 2nd peaks were generated.

Figure S2(b) shows the corresponding temporal waveform for the 2nd peak condition. In the temporal domain, the spectral peak was broad, weak pulse and the ultrashort pulse was overlapped on it. When the fiber length was 5 m, the ultrashort pulse spectrum was temporally broadened to 2.4 ps, and it induced the cross-phase modulation (XPM) on the spectral peak. In Fig. S2(b), we can see the modulation on the temporal waveform of ultrashort pulse by XPM. As the result, the spectral peak components were slightly broadened towards both sides. The temporal part overlapped with the leading edge of the ultrashort pulse was red-shifted, and that with the trailing edge was blue-shifted. These XPM components interfered with the spectral envelope, and induced the dips and small bumps around the spectral peak. These spectral dips contributed to the enhancement of the SBR for these spectra.

S3. Temporal profiles of multiple spectral peaks

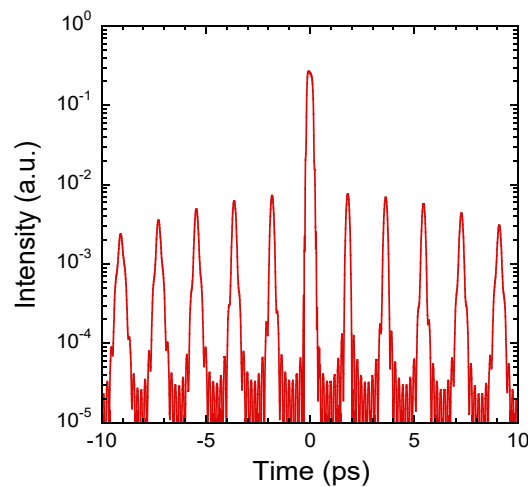


Fig. S3. Temporal waveform of 10 spectral peaks with 5 nm separation.

Figure S3 shows the numerically obtained temporal waveform of the optical pulse, which corresponds to the 10 spectral peaks with 5 nm separation shown in Fig. 6(a). The pulse train with 1.9 ps constant interval with high contrast was clearly observed. The power level of the pulse train was $-18 \sim -20$ dB from the main pulse. We can see that the ultrahigh repetition rate pulse train was generated from the multiple spectral filtering. The pulse energy was dispersed into the sub-pulses around the main pulse.

S4. RF noise properties

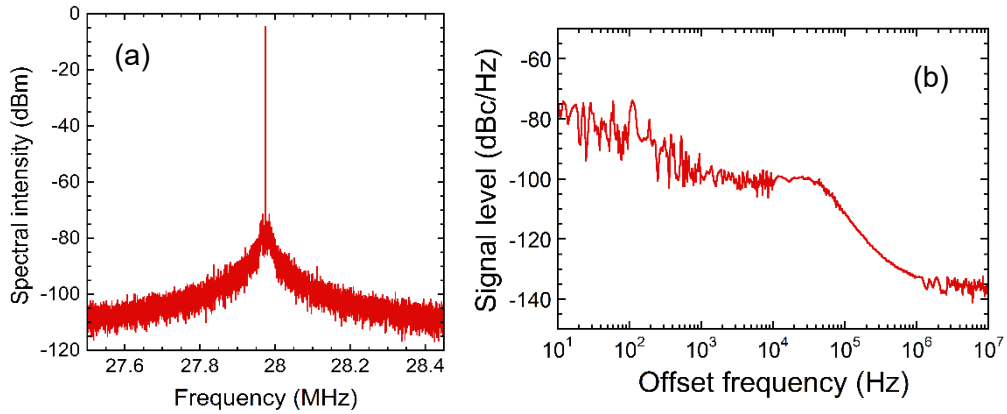


Fig. S4. (a) RF spectra and (b) phase noise of one extracted peak.

We also examined the RF spectra and phase noise of the spectral peak. Here only the single extracted peak was radiated on a fast pin photo-diode, and RF signals were observed. As shown in Fig. S4(a), a very clean RF spectrum was observed, and the SNR was up to 70 dB.

Figure S4(b) shows the phase noise observed using an RF spectrum analyzer (Anritsu MS2830A). We used the optional function for phase noise measurement in the RF spectrum analyzer. From Fig. S4, we confirmed that both the noise level and phase noise were low, and they were not increased for the spectral peak component.

In our previous work [5], we observed the RF beat between the generated spectral peak and stable cw-LD. The RF beats were observed with a high SNR of ~ 50 dB, and a comb structure with a high SNR was confirmed.

From these experiments, and considering the physical mechanism, it is considered that the spectral peak component retains the coherence properties of the passively mode-locked fs ultrashort pump pulses.

During the experiment, the generated spectral peaks showed a good long-term stability.